Paulo Magalhaes Martins*, Riccardo Dal Bello, Andreas Rinscheid, Katja Roemer, Theresa Werner, Wolfgang Enghardt, Guntram Pausch, and Joao Seco

Prompt gamma spectroscopy for range control with $CeBr_3$

Abstract: The ultimate goal of radiotherapy using external beams is to maximize the dose delivered to the tumor while minimizing the radiation given to surrounding healthy critical organs. Prompt Gamma Spectroscopy (PGS) has been proposed for range control of particle beams along with the determination of the elemental composition of irradiated tissues. We aim at developing a PGS system for the German Cancer Research Center – DKFZ that takes advantage of the superior selectivity of Helium and Carbon beams accelerated at the Heidelberg Ion-Beam Therapy Center. Preliminary tests with protons accelerated with an IBA C230 cyclotron located at the *Universitäts Protonen Therapie Dresden* were performed at OncoRay – National Center for Radiation Research in Oncology. We present results obtained with a PGS system composed of $CeBr_3$ detectors (∅ 2'' × 2'') and (∅ 1.5'' × 3'') coupled to a Hamamatsu R13089 photomultiplier tube and plugged to a Target U100 Spectrometer. Such system provides accurate time-of-flight measurements to increase the signal-to-noise ratio relative to neutron-induced background. First measurements resulted from the irradiation of PMMA and water phantoms, and graphite and aluminum bricks. Several PG energy lines ranging from 0.511 MeV up to 8 MeV were identified and compared with reference results. Two further experiments consisted in irradiating PMMA phantoms in a slit- and semi-collimated configuration with mono-energetic proton beams of 165 MeV and 224 MeV, respectively. Results acquired by means of transversal PGS at different phantom depths, ranging from 6 cm before the Bragg peak (BP) to 3.5 cm beyond the BP in 5 mm steps with a 1 cm slit collimation (tungsten) showed a slight decrease of PG yields after the BP. Similar measurements with a semi-opened collimation configuration demonstrated a steeper decrease of PG yields after the BP.

Keywords: cerium-bromide, prompt-gamma, time-of-flight, proton therapy, range verification, gamma-ray spectrometer

https://doi.org/10.1515/cdbme-2017-0023

***Corresponding author: Paulo Magalhaes Martins:** German Cancer Research Center, Im Neuenheimer Feld 280,69120 Heidelberg, Germany, e-mail: p.martins@dkfz.de; Institute of Radiooncology, Helmholtz-Zentrum Dresden-Rossendorf, Fetscherstrasse 74, 01307 Dresden, Germany; Institute of Biophysics and Biomedical Engineering (IBEB), Faculty of Sciences of the University of Lisbon, Lisbon, Portugal
Joao Seco: German Cancer Research Center, Im Neuenheimer Feld 280,69120 Heidelberg, Germany, e-mail: j.seco@dkfz.de; Department of Physics and Astronomy, University of Heidelberg, Heidelberg, Germany
Riccardo Dal Bello: German Cancer Research Center, Im Neuenheimer Feld 280,69120 Heidelberg, Germany, e-mail: r.dalbello@dkfz.de; Max Planck Research School, Quantum Dynamics, Heidelberg, Germany
Wolfgang Enghardt: German Cancer Research Center, Im Neuenheimer Feld 280,69120 Heidelberg, Germany; Institute of Radiooncology, Helmholtz-Zentrum Dresden-Rossendorf, Fetscherstrasse 74, 01307 Dresden, Germany; OncoRay – National Center for Radiation Research in Oncology, Faculty of Medicine and University Hospital Carl Gustav Carus, Technische Universität Dresden, Helmholtz-Zentrum Dresden- Rossendorf, Dresden, Germany, e-mail: Wolfgang.Enghardt@oncoray.de; German Cancer Consortium (DKTK), Dresden, Germany,
Andreas Rinscheid: Institute of Physics, Martin Luther University, Von-Danckelman-Platz 3, 06120 Halle (Saale), Germany, e-mail: a.rinscheid@gmail.com
Katja Roemer: Institute of Radiation Physics, Helmholtz-Zentrum Dresden-Rossendorf, Bautzner Landstraße 400, 01328 Dresden, Germany, e-mail: Katja.Roemer@oncoray.de
Theresa Werner and Guntram Pausch: Institute of Radiooncology, Helmholtz-Zentrum Dresden-Rossendorf, Fetscherstrasse 74, 01307 Dresden, Germany, e-mail: theresa.werner@oncoray.de; guntram.pausch@oncoray.de

1 Introduction

Over the last 25 years, millions of euros/dollars were spent without any successful solution to proton range errors [1]. The major consequence of these range errors is that significantly larger high dose regions are created around the tumor with severe consequences to the patient.

Prompt gamma imaging (PGI) has been proposed as a superior method to Positron Emission Tomography (PET) for range verification, with the potential to achieve 1 mm uncertainty in the positioning of the Bragg peak within the patient [2]. PGI allows real-time range verification and does not

suffer from biological washout or motion effects. In addition, a significantly higher PG production and closer correlation with dose profiles due to higher cross-sections makes it more attractive than PET.

A novel approach for measuring prompt gammas, combining energy- and time-resolved detection has been proposed by Verburg and Seco [3]. Besides using the prompt gamma signal for range verification, the emitted gamma spectrum allows determining the elemental composition of irradiated tissue.

The characterization of $CeBr_3$ detectors for usage as PG monitors in particle therapy has been firstly accomplished by Römer et al. [4]. Such detectors were systematically investigated by Pausch et al. [5] and firstly applied to prompt gamma timing (PGT). In this work, we propose to use $CeBr_3$ scintillators for prompt gamma spectroscopy (PGS).

2 Materials and methods

2.1 Experimental setups

The measurements were divided in three campaigns. In the first campaign, Water and PMMA phantoms and a Graphite Brick were irradiated with a mono-energetic proton beam of 130 MeV. For the Aluminium brick we adjusted the energy to 90 MeV.

The schematics of the experimental setup is depicted in Figure 1a). The detection system was composed of a $CeBr_3$ detector (∅ 2'' × 2'') coupled to a Hamamatsu R13089 photomultiplier tube and plugged to a Target U100 Spectrometer [6].

The system was located at 90º with respect to the beam, at a distance of 50 cm and aligned with the Bragg peak position. The energy spectrum was calibrated with a ^{22}Na source and the photomultiplier voltage was adjusted accordingly.

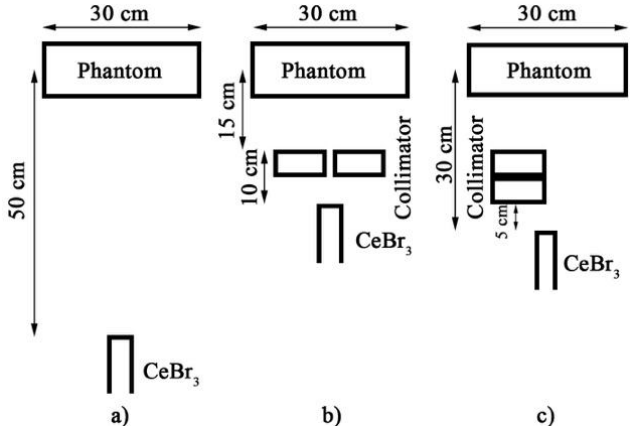

Figure 1: Schematic drawing of the three campaigns for the prompt gamma acquisition from proton-irradiated phantoms using: a) no collimation; b) slit collimation; c) semi-collimation.

In the second campaign, a tungsten collimator with a thickness of 5 cm was placed between the PMMA phantom and the detecting system. The scheme is shown in Figure 1b). The phantoms were placed on a moving platform and displaced in 5 mm steps covering a region from 6 cm before the BP up to 3.5 cm after the BP.

In the last campaign, we used different $CeBr_3$ detectors (∅ 1.5'' × 3'') and doubled the collimator thickness in a semi-collimation configuration, see Figure 1c). We also acquired for several detector positions along the beam range covering a region from 9 cm before the BP until 9 cm after the BP. We irradiated a PMMA phantom with the maximum energy available – 224 MeV. Figure 2 shows a photograph of the setup in campaign 2 and 3. We set a beam current of 0.4 nA measured at the ionization chamber and an acquisition time of 50 s for both campaigns. The observed throughput rates for the 3 campaigns varied between 300 and 500 kcps with a busy time of 30-50% as indicated by the U100.

The spectrometer streamed acquired data in list-mode format to a server which then saved them in binary files containing the time stamp (64-bit integers) and the energy information (32-bit floats). This data was further analysed with MATLAB and ROOT (version 5.34.00, CERN, Geneva, Switzerland). The accelerator radio-frequency (RF) has been used for timing information as external reference clock. The detailed specifications of the detection system are reported in a more comprehensive work [5].

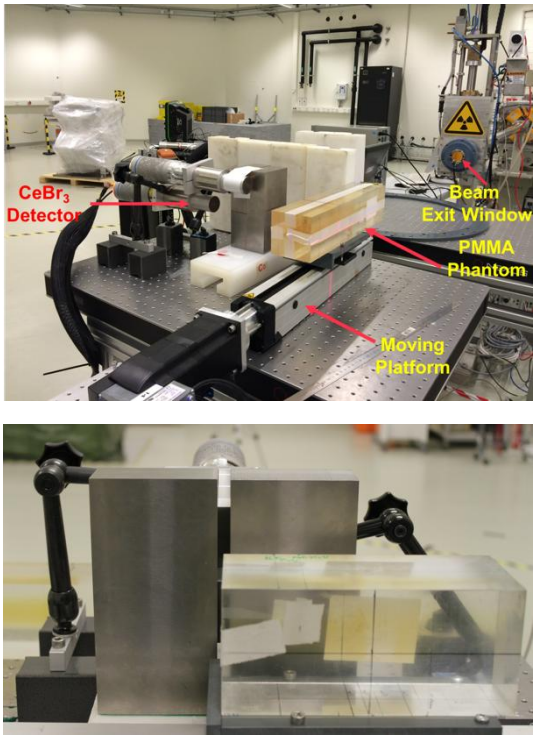

Figure 2: Photos of campaign 2 (bottom) – slit collimation, and 3 (top) – semi-collimation.

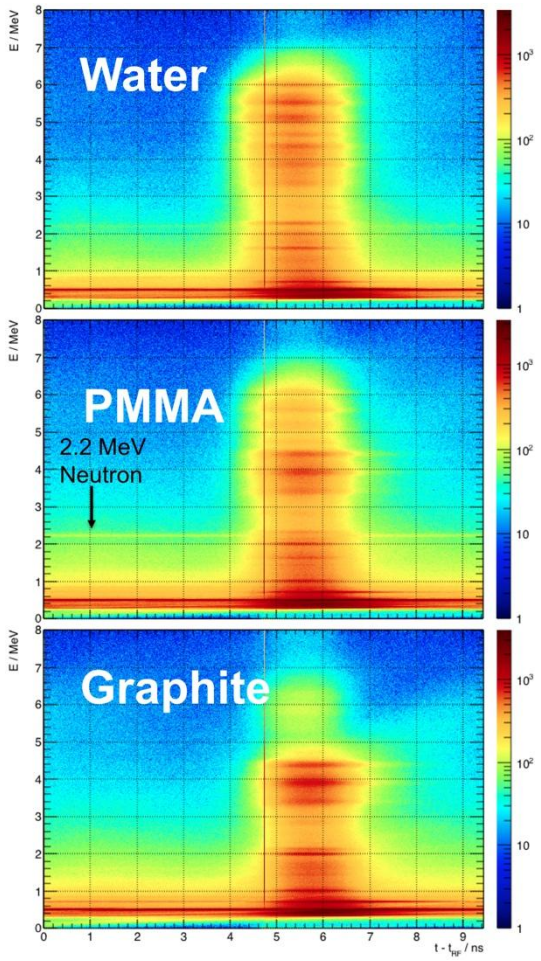

Figure 3: Prompt gamma lines and corresponding single- and double-escape peaks visible as time correlated horizontal stripes. The targets were irradiated with a mono-energetic proton beam of 130 MeV in a setup without collimation.

3 Results

3.1 No collimation

Figure 3 shows a 2D histogram with the energy- and time-resolved prompt gammas emitted from water, PMMA and graphite targets irradiated in campaign 1, see Figure 1a). The prompt gamma lines and corresponding single- (SE) and double-escape (DE) peaks are visible as horizontal stripes. Several time-uncorrelated lines are also visible (e.g., the 511 keV line from positron annihilation and the 2.2 MeV line resulting from hydrogen neutron capture).

3.1.1 Energy spectra

Figure 4 shows the energy spectra within 5 ns and 6 ns for the water (I) and PMMA (II) phantoms and the graphite (III) brick irradiated in campaign 1, see Figure 1a). The energy peaks are related to reactions with material nuclei or characteristic transitions from excited states as a result of the interaction with the proton beams. In table 1, we identified 17 transitions or reactions for the three irradiated materials (targets) and compared with the reference values [7].

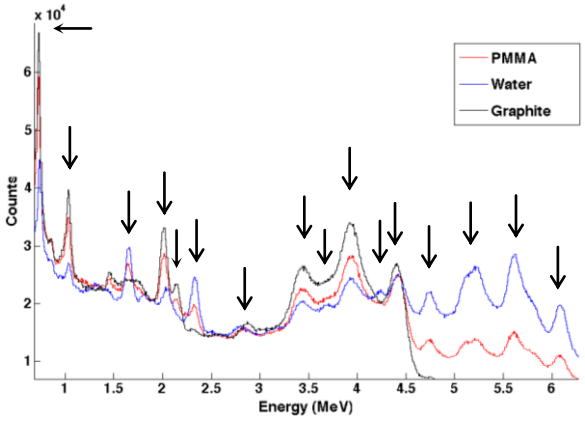

Figure 4: Energy spectra corresponding to prompt-gamma rays resulting from the irradiation of PMMA, water and graphite for the interval 5-6 ns.

Table 1: Comparison of measured energy peaks for characteristic transitions/reactions with reference values.

Transition/Reaction	Target	Reference Line (MeV)	Measured (MeV)
β-decay	I,II,III	0.511	0.509
$^{10}B^{*0.718}$-> g.s. / $^{12}C(p,x)^{10}B^{*}$	I,II,III	0.718	0.718
$^{10}B^{*1.740}$-> $^{10}B^{*0.718}$ / $^{12}C(p,x)^{10}B^{*}$	I,II,III	1.022	1.028
$^{14}N^{*3.948}$-> $^{14}N^{*2.313}$ / $^{16}O(p,x)^{14}N^{*}$	I,II	1.635	1.636
$^{11}C^{*2.000}$-> g.s. / $^{12}C(p,x)$ $^{11}C^{*}$	I,II,III	2.000	2.012
$^{11}B^{*2.125}$->g.s. / $^{12}C(p, x)^{11}B^{*}$	I,III	2.124	2.124
$^{14}N^{*2.313}$-> g.s. / $^{16}O(p,x)^{14}N^{*}$	I,II	2.313	2.324
$^{16}O^{*8.872}$-> $^{16}O^{*6.130}$ / $^{16}O(p,p')^{16}O^{*}$	I,II	2.742	2.788
$^{12}C^{*4.439}$-> g.s. / $^{12}C(p,p*)^{12}C^{*}$	I,II,III	3.416	3.436
$^{13}C^{*3.685}$-> g.s. / $^{16}O(p,x)^{13}C^{*}$	II	3.684	3.684
$^{12}C^{*4.439}$-> g.s. / $^{12}C(p,p*)^{12}C$	I,II,III	3.927	3.924
$^{15}N^{*5.181}$-> g.s. / $^{16}O(p,x)^{15}O^{*}$	II	4.158	4.167
$^{12}C^{*4.439}$-> g.s. / $^{12}C(p,p*)^{12}C^{*}$	I,II,III	4.438	4.427
$^{15}N^{*5.270}$-> g.s. / $^{16}O(p, x)^{15}N^{*}$	I,II	4.758	4.756
$^{15}N^{*5.181}$-> g.s. / $^{16}O(p,x)^{15}O^{*}$	I,II	5.180	5.204
$^{16}O^{*6.130}$-> g.s. / $^{16}O(p,p')^{16}O^{*}$	I,II	5.618	5.612
$^{16}O^{*6.130}$-> g.s. / $^{16}O(p,p')^{16}O^{*}$	I,II	6.129	6.076

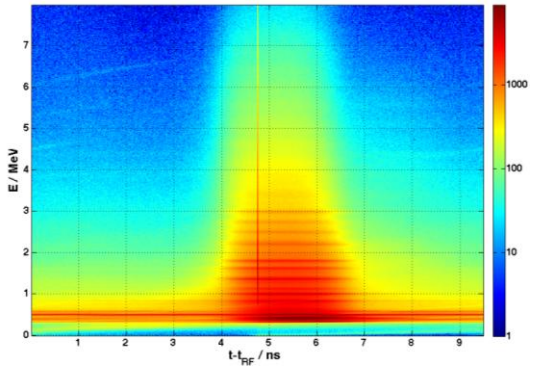

Figure 5: Prompt gamma lines resulting from the irradiation of Aluminium with protons (E = 90 MeV).

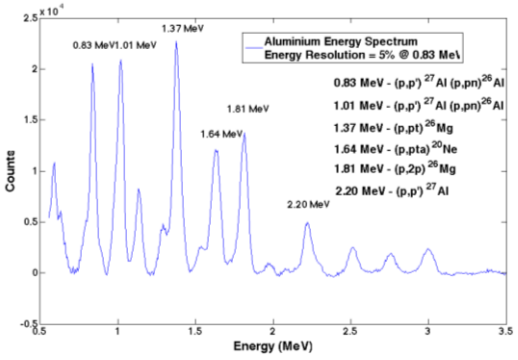

Figure 6: Energy spectrum corresponding to prompt gamma-rays from proton irradiation of aluminium. The six reactions that are believed to be responsible for their production are also shown.

3.1.2 Metal spectroscopy

Several metals are used as implants in orthopaedics and dentistry. They are mainly made of titanium and gold and affect the proton range due to their high stopping power. Prompt gamma spectroscopy may have a role in the range ber. Figure 5 shows the prompt gamma lines resulting from the irradiation of an Aluminium brick with a proton beam with an energy of 90 MeV. The energy spectrum for the interval 5-6 ns is show in Figure 6. The energy peaks agree with the values reported by Foley et al [8].

3.2 Slit collimation and semi-collimation

Figure 7 shows the prompt-gamma lines from a slit collimated configuration for an interval of 1.5 ns and at different positions before and after the BP (5 mm steps). The event counts are represented in logarithmic scale (top). An energy-cut in lines below 2 MeV was applied in the linear-scaled histogram (bottom) for better visualisation. It clearly shows the 4.4 MeV line from carbon deexcitation and corresponding SE and DE peaks. As expected, those are the most intense

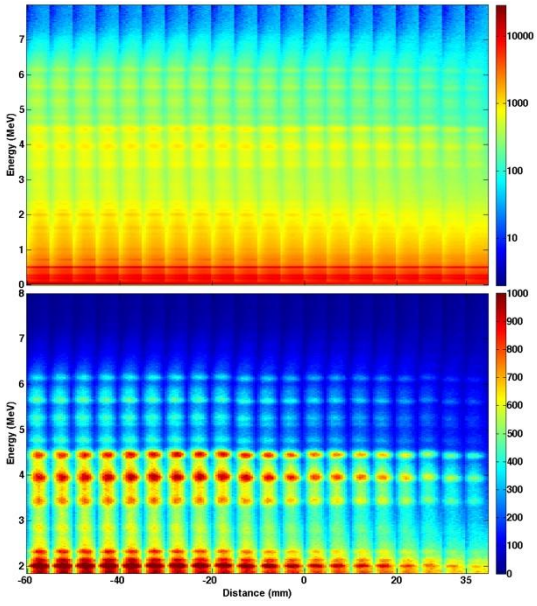

Figure 7: Energy lines of slit-collimated prompt-gammas resulting from the irradiation of PMMA with protons (E = 165 MeV) along 20 positions before and after the BP (zero). Top: Logarithmic scale, full energy range. Bottom: Linear scale, energy cut at 2 MeV.

lines and a reduction in the prompt gamma yields after the BP is observed.

Figure 8 shows the prompt-gamma lines from a semi-collimated configuration for the same time interval at 25 positions before and after the BP. The linear histogram (bottom) shows a steeper decrease of the prompt gamma yields

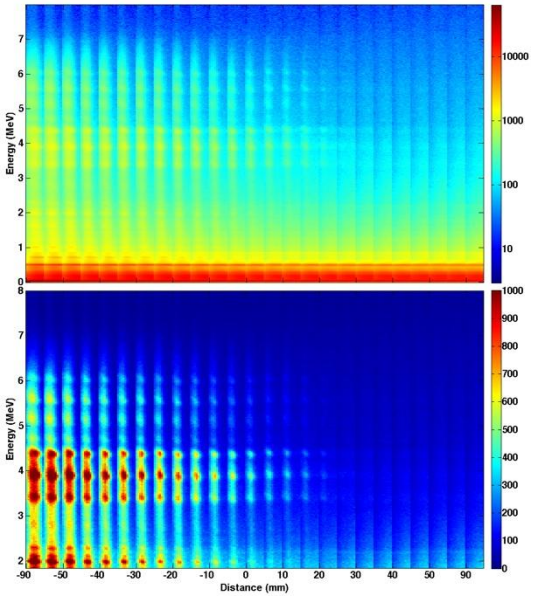

Figure 8: Energy lines of semi-collimated prompt-gammas resulting from the irradiation of PMMA with protons (E = 224 MeV) along 25 positions before and after the BP (zero). Top: Logarithmic scale, full energy range. Bottom: Linear scale, energy cut at 2 MeV.

after the BP than with the slit collimation. This may be due to the thickness of the collimator, which lets a fraction of gamma-rays through it.

4 Discussion

We accomplished three campaigns, where several materials have been irradiated with proton beams in the energy range from 90 to 224 MeV. In the first campaign, we had no collimator between the target and the detection system. Due to the good TOF capabilities of this system, we observed an energy-time correlation of prompt-gammas. This allowed the subsequent time window selection with a significant reduction of background events and the identification of prompt-gamma lines. Time-uncorrelated energy lines were also observed. We also observed that the energy spectra corresponding to prompt gamma-rays from the irradiation of Water and PMMA phantoms and a graphite brick shows a significant agreement within the energy peaks positions. A total of 17 reactions or transitions that are believed to be responsible for the production of such prompt-gamma rays were identified and compared with reference values. Moreover, six additional reactions were identified from the irradiation of an Aluminium brick. This may open doors for the application of this system in clinical scenarios where metal implants of high-*Z* materials, such as titanium and gold, are present. We performed 2 further campaigns with slit- and semi-collimation configurations. The third campaign had doubled tungsten collimator thickness in comparison with the second campaign, which contributed to the better efficacy in the collimation and therefore a steeper gradient in the number of detected prompt-gammas after the BP. Some residual prompt-gamma detection was observed with a higher prominence for the 4.4 MeV and SE and DE peaks. Such geometry coupled with such detection system seems to be promising in the range control of particle beams through PGS. Future work includes the implementation of an active anti-coincidence shielding for background reduction and the systematic comparison of different detector sizes for an optimized prompt-gamma data collection.

Acknowledgment
The authors would like to thank the support from Ion Beam Applications S.A. (IBA).

Author's Statement
Research funding: The authors state no funding involved. Conflict of interest: Authors state no conflict of interest. Informed consent: Informed consent is not applicable. Ethical approval: The conducted research is not related to either human or animals use.

References

[1] Knopf AC, Lomax A. In vivo proton range verification: a review. Phys Med Biol 2013; 58:131-160.
[2] Moteabbed M, España S, Paganetti H. Monte Carlo patient study on the comparison of prompt gamma and PET imaging for range verification in proton therapy, Phys Med Biol 2011; 56:1063-1082.
[3] Verburg JM, Seco J, Prompt range verification through prompt gamma-ray spectroscopy. Phys Med Biol 2014; 59:7089-7106
[4] Roemer K, Pausch G, Bemmerer D et al. Characterization of scintillator crystals for usage as prompt gamma monitors in particle therapy. JINST 2015, 10:P10033
[5] Pausch G, Petzold J, Berthel M et al. Scintillator-based high-throughput fast timing spectroscopy for real-time range verification in particle therapy. IEEE Trans Nucl Sci 2016; 63:664:672
[6] Target Systemelektronik GmbH & Co. KG, http://target-sg.com/
[7] Kozlovsky B, Murphy RJ, Ramaty R. Nuclear deexcitation gamma-ray lines from accelerated particle interactions. The Astrophysical Journal Supplement Series 2002; 141:523:541
[8] Foley KJ, Clegg AB, Salmon GL. Gamma-radiation from the medium energy proton bombardment of Sodium, Magnesium, Aluminium, Silicon, phosphorus and Sulphur. Nucl. Phys. 1962; 37:23-44.